The International Journal of Advanced Manufacturing Technology (2018) 97:599–609
https://doi.org/10.1007/s00170-018-1938-5

ORIGINAL ARTICLE

Error analysis of high-speed precision micro-spindle equipped with micro-tool in mechanical micro-grinding

Wei Li[1] · Zhipeng Li[1] · Yinghui Ren[1] · Xiangming Huang[1]

Received: 4 December 2017 / Accepted: 20 March 2018 / Published online: 7 April 2018

Abstract
The existing micro-spindle systems equipped with micro-tools compromise micro-machining accuracy and efficiency due to their large error. In this study, the radial error of micro-tool tip was classified into static mechanical offset, thermally induced error, and radial motion error. The micro-tool tip, having the smallest stiffness, was the major error source of radial mechanical offset. A stiffness-based error model was proposed to predict the radial mechanical offset of micro-tool tip, and the predictions were well consistent with the measured values. The front bearing, due to its large thermal loss, had lower temperature than the rear bearing at nearly all rotational speeds. The difference of thermal growths between the two ball bearings resulted in the thermally induced error. The thermally induced error increased rapidly with running time within the first hour and then entered into a relative stable state, which was modeled by the least square method. The proposed model of thermally induced error also considered exponential characteristic of spindle thermal growth in nature. It agreed well with the measured values. The radial motion error increased with the over-hang length of micro-tool, but decreased with the rotational speed. It was modeled by the least square method and validated by the measurements. The micro-grinding tests were conducted to further verify the proposed predictive models of static mechanical offset, thermally induced error, and radial motion error. With the error compensation, the micro-grinding thickness was close to the required value, which showed the error predictive models and compensation scheme were effective.

Keywords Micro-spindle · Micro-grinding tool · Motion error · Thermally induced error · Micro-grinding

1 Introduction

The miniaturization of products not only decreases weight, but also possesses more functions. This trend has created tremendous demand for micro/mesoscale parts and components in many fields such as aerospace, defense, optics, electronics, and biomedicine. Therefore, researches and technological developments in micro-manufacturing and fabricating of precision micro-scale features on metals, polymers, ceramics, glasses, and composites have attracted increasing attention [1]. Techniques including laser beam machining, ion beam machining, electro-discharge machining (EDM), and electrochemical machining (ECM) have been successively developed based on energy beam, physical, and chemical effects [2]. These methods mainly concentrate on the silicon machining and are limited to plane geometries; therefore, they are typically used as "silicon-based machining techniques" in electronics industry. Another micro-manufacturing process is mechanical micro-machining, including micro-turning, micro-milling, micro-drilling, and micro-grinding [3]. Their micro-tools are in direct mechanical contact with the workpieces, which can provide a good geometric correlation between the micro-tool and machining surface. Therefore, the mechanical micro-machining has advantages in machining three-dimensional intricate micro/mesoscale features and parts on a broad range of materials [4]. When the miniature machine tools equipped with high-speed micro-spindle are adopted, high material removal rates, small volume, and energy consumption can be realized.

Since the micro-tools, such as micro-milling tools and micro-grinding tools with a tool body diameter of 3 mm or 0.125 in. and a tool tip diameter of less than 1 mm, are directly mounted into micro-spindles, their machining accuracy and efficiency are closely related to micro-spindles. In recent

✉ Wei Li
liwei@hnu.edu.cn

[1] College of Mechanical and Vehicle Engineering, Hunan University, Changsha 410082, China

years, in conjunction with higher performance, more functions, and smaller size of products, the level of mechanical micro-machining is expected to be further advanced. To this end, efforts are being made to develop high-speed precision micro-spindles. In terms of dimensional and form accuracy of submicron, the micro-spindle should satisfy at least the requirement of commensurate motion error. For micro-parts of submillimeter, the motion error of less than 100 nm is required [5]. In addition, the micro-tool is less than 1 mm in tip diameter; therefore, the micro-spindle must provide ultra-high speed to attain desired cutting speed. Müller et al. [6] reviewed a series of newly developed spindles for mechanical micro-machining and compared their performances. Some newly developed micro-spindles can be operated at a high rotational speed up to 500,000 rpm [6, 7], but unfortunately, the desired accuracy cannot be obtained. A few commercially available micro-spindles, with a maximum rotational speed of less than 200,000 rpm, achieve the spindle accuracy within 1 μm. However, the radial motion error of the attached micro-tools varies with the spindle speed and may exceed 1 μm. Our research team proposed a monolithic flexible coupling to decouple the spindle shaft from micro-tool and then supported the tool shank by aerostatic bearings. Due to the limitation of manufacturing accuracy, the developed micro-spindle reached 240,000 rpm, with a tool motion error of 2.79 μm [6, 8, 9]. Therefore, efforts are still needed to further reduce the error motion of micro-spindles especially at ultra-high speeds. This means that up to now, the large error of high-speed micro-spindles during the design and manufacturing phase has not been solved yet. Therefore, it is of great significance to ascertain the error source and then propose a corresponding compensation scheme for improving the level of mechanical micro-machining.

In reality, the micro-tool tip is in direct mechanical contact with the workpiece during mechanical micro-machining. Accordingly, the dimensional accuracy, form accuracy, and surface roughness are critically affected by the error of micro-tool tip. In addition to the error motion of the micro-spindle and the thermal error arising from heat-up of build-in motor's power loss and friction of bearings, the centering error and profile error of micro-tool may also contribute to the undesired error of the micro-tool tip during mechanical micro-machining. Ashok et al. [10] proposed a capacitive sensor-based measurement technique to assess the radial errors of a miniaturized machine tool spindle, finding that the asynchronous radial error motion exhibited a significant speed-dependent behavior which did not exist in synchronous radial error motion. Murakami et al. [11] presented an optical technique and measured the error motion of a high-speed micro-spindle. Anandan et al. [12] presented a LDV-based methodology for measurement of axial and radial error motions of ultra-high-speed miniature spindles and concluded that the average radial motion, synchronous radial error motion, and standard deviation of asynchronous radial error motion varied significantly with the spindle speed. These different findings may contribute to the development of different miniature spindles. However, further investigations beyond the scope of current work are still needed. Bediz et al. [13, 14] investigated the dynamics of micro-tools and miniature ultra-high-speed spindle, finding that the spindle speed had a significant effect on dynamic response whereas the collet pressure did not have. Creighton et al. [15] ascertained the displacement of the micro-tool tip caused by thermal error and presented a spindle growth compensation scheme to reduce the thermally induced mechanical micro-milling error. Anandan et al. [16] investigated the effects of more factors including thermal cycling, spindle speed, over-hang length, and repeatability of artifact attachment on the radial and axial error motions of miniature ultra-high-speed spindle. They pointed out the error motion was strongly dependent upon the speed, thermal state, and over-hang of the artifact (tool), and concluded that any error arising from tool, collet, and spindle may all be reflected at the micro-tool tip, which means that the error of micro-tool tip may be the comprehensive embodiment of these errors. Accordingly, comprehensive error analysis of the tool-collet-spindle system can provide more quantitative understanding of the error effect of high-speed precision micro-spindle equipped with micro-tool on mechanical micro-machining accuracy. Establishing a compensation scheme is very essential for improving the accuracy and efficiency of mechanical micro-machining. However, there have been few studies on performing comprehensive error analysis to specifically understand and quantify the error sources contributing to the error of micro-tool tip. Uriarte et al. [17] established the error budget for the micro-tool tip based on the stiffness chain including stiffnesses of machine, spindle, collet, and tool itself and concluded that the micro-tool with a diameter of less than 0.3 mm was the most flexible element. However, their study only aimed at static offset error of micro-tool mounted into the conventional spindle.

In this study, the comprehensive error analysis was conducted to quantify various error sources contributing to the error of micro-grinding tool tip driven by high-speed precision micro-spindle. The stiffness model of the tool-collet-spindle system was established to obtain the mechanical offset of micro-tool tip. The thermally induced error and motion error of the micro-spindle were measured, and their relations with rotational speed and over-hang length of micro-tool were modeled. Then, an error analysis-based compensation scheme was proposed. Finally, such compensation scheme was applied to mechanical micro-grinding to verify its effectiveness in improving the accuracy of mechanical micro-machining.

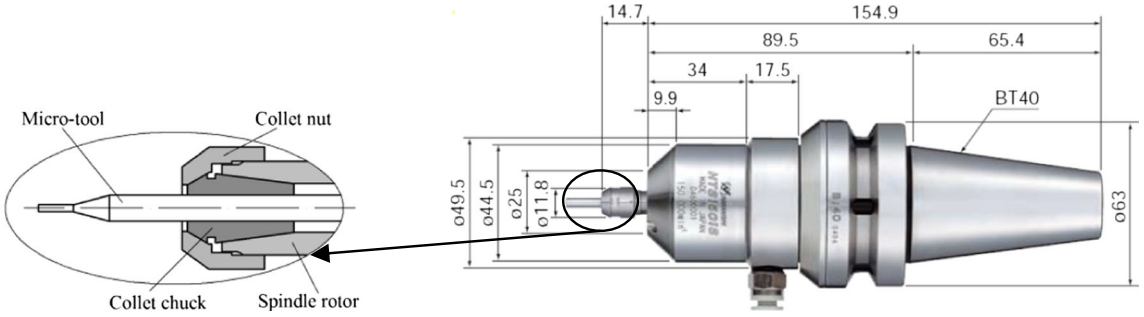

Fig. 1 Air turbine spindle

2 Error analysis of micro-tool tip

The factors affecting the offset of micro-tool tip are generally regarded as the error sources, which should be first identified and then quantified. The micro-spindle used in this study is HTS1501S-BT40 air turbine spindle (Nakanishi Inc.), which achieves a maximum rotational speed of 150,000 rpm and a spindle runout within 1 μm, as shown in Fig. 1. The micro-tool used in this experiment is a commercially available micro-grinding tool, with 0.3 mm in tool tip diameter, 3 mm in tool body diameter, and 35 mm in overall length, as shown in Fig. 2. During micro-grinding, the grinding force causes the offset of micro-tool tip due to the small stiffness of tool-collet-spindle-bearing system, which was classified into the mechanical offset in this study. After long-time running, the micro-spindle generates heat and results in thermally induced error. Moreover, the spindle runout and resulted machining error are also inevitable.

2.1 Mechanical offset

The micro-spindle system consists of spindle rotor, bearings, collet, and micro-tool. The radial offset of any of these components can cause the offset of micro-tool tip. Therefore, the radial offset of micro-tool tip is a systematic accumulative error. According to related theory of material mechanics, the radial error diagram of micro-tool tip can be drawn, as shown in Fig. 3. The corresponding radial offset of micro-tool tip U_g can be expressed as Eq. (1).

$$U_g = \sum \delta_i = \delta_{sp} + \delta_c + \delta_t \tag{1}$$

where δ_{sp}, δ_c, and δ_t are radial offsets of micro-spindle, collet, and micro-tool, respectively. The model above directly reflects the radial offset of micro-tool tip. However, it is inconvenient to evaluate the radial offset of micro-tool tip at various grinding forces using this model. As this tool-collet-spindle-bearing system is actually a series system, the stiffness-based model for evaluating radial offset of micro-tool tip was proposed as Eq. (2). Since the radial offset of micro-tool tip attracts more concern, the radial offset and corresponding stiffness were deeply analyzed in this study.

$$\frac{1}{K_g} = \frac{1}{k_{sp}} + \frac{1}{k_c} + \frac{1}{k_t} \tag{2}$$

where K_g, k_{sp}, k_c, and k_t are stiffnesses of tool-collet-spindle system (i.e., global stiffness), micro-spindle, collet, and micro-tool, respectively.

2.1.1 Deflection of micro-tool and its stiffness

Although the micro-tool body is typically 3 mm in diameter, its tool tip is less than 1 mm. At present, the commercially available micro-grinding tools have a minimum tool tip diameter of 0.3 mm, as shown in Fig. 2b. As the deflection is large relative to the precision requirement of submicron, the deflection of the micro-tool is an important error source. The micro-tool tip was loaded by small weights and its deflection was measured by MTI-2100 fotonic sensor, as shown in Fig. 4. This sensor is a fiber-optical measuring system, with maximum resolution of 2.5 nm and maximum frequency response of 50,000 Hz. Figure 5 shows the measured results, from which it can be seen that the radial displacement linearly increased with the load,

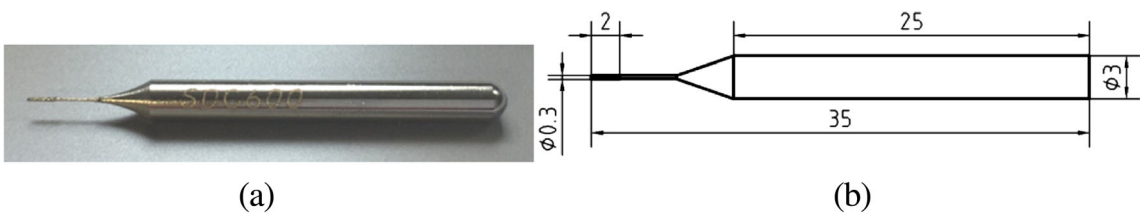

Fig. 2 Micro-grinding tool (**a**) and its dimensions (**b**)

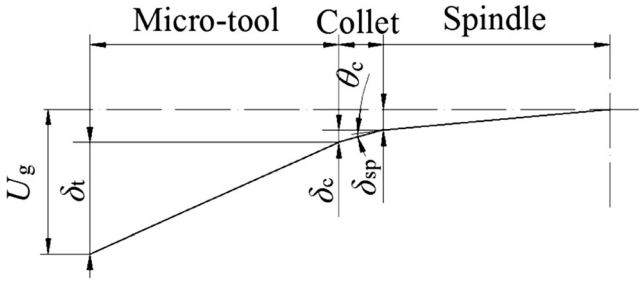

Fig. 3 Radial error diagram of micro-spindle system

and the maximum displacement reached 10.3 μm under a load of 2 N. The stiffness of micro-grinding tool tip is 195.0 mN/μm. It should be noted that during measuring the stiffness of tool tip, the whole tool body was fixed. The conical part of the tool (Fig. 2) did not get in touch with the fixture and thus was not fixed. Consequently, the obtained stiffness of tool tip included that of the conical section of the tool.

In this experiment, it was difficult to apply a load onto the micro-tool tip. There was a distance a between the measured point where the force was applied and the free end; therefore, the obtained stiffness needed to be further corrected [17]. According to material mechanics theory, when the cantilever beam is subjected to a concentrated force F, its deflection y at a distance b is

$$y = \frac{Fb^2(3L-b)}{6EI} \tag{3}$$

where E is elastic modulus, I is inertia moment, L is length, and $b = L - a$.

Accordingly, the correction coefficient can be obtained by

$$\alpha = \frac{\frac{Fb^2}{6EI}(3L-b)}{\frac{FL^3}{3EI}} = \frac{b^2(3L-b)}{2L^3} \tag{4}$$

The measuring parameters are shown in Table 1. According to above correction model, the stiffness of micro-grinding tool tip was 171.6 mN/μm. In addition, the stiffness of the tool body was also measured in the same way. The radial displacement under a load of 2 N was 0.8 μm. The stiffness of tool body was about 2524.3 mN/μm, which is much larger than that of tool tip, indicating that the tool tip is a dominant factor for evaluating the mechanical offset of micro-tool.

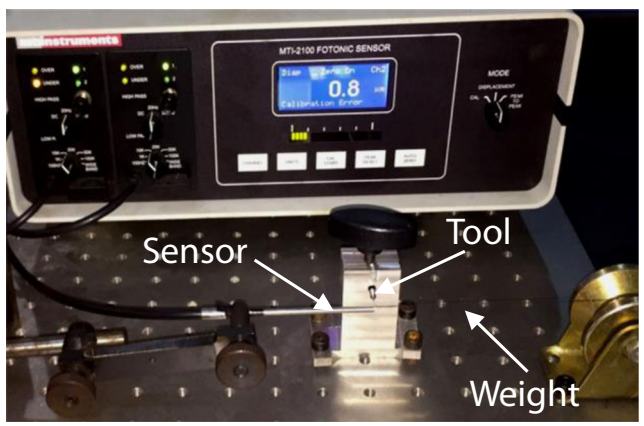

Fig. 4 Measurement for the stiffness of micro-grinding tool

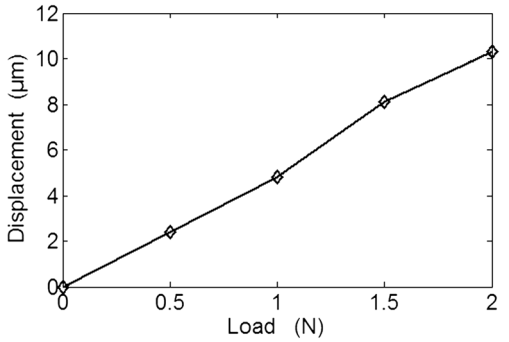

Fig. 5 Radial displacement of micro-grinding tool tip

2.1.2 Stiffness of collet

In the micro-spindle system used for micro-milling or micro-grinding, the collet is typically attached to the spindle rotor (Fig. 1); therefore, the spindle/tool shank section was not considered in this study. Since it was inconvenient to apply a load on the end of the collet, the load was applied to the tool body which is very close to the collet. Moreover, the spindle rotor near the other end of the collet was supported. When a load of 0–4 N was applied, the resultant radial displacement was 0–0.55 μm. Therefore, the radial stiffness of the collet k_c is approximately 7157.5 mN/μm.

In addition, the angular deformation resulting from the rotation of the collet can also cause the radial offset of the tool tip (Fig. 3). Since the deformation can be amplified by the distance between the collet and tool tip [18], its angular stiffness needs to be ascertained. To calculate the angular stiffness of collet, a load F was applied onto the tool body, and the radial displacements at two points were measured, as shown in Fig. 6. Based on the theory of material mechanics, the angular stiffness k_θ is given by Eq. (5).

$$\begin{aligned} k_\theta &= \frac{M_c}{\theta_c} \\ M_c &= F \cdot L_F \\ \theta_c &= \arctan\left(\frac{u_d - u_c}{d-c}\right) \end{aligned} \tag{5}$$

Table 1 Parameters for stiffness calculation of micro-grinding tool tip

Tip, Ø (mm)	L (mm)	a (mm)	α	Stiffness (mN/μm)
0.3	6	0.5	0.88	171.6

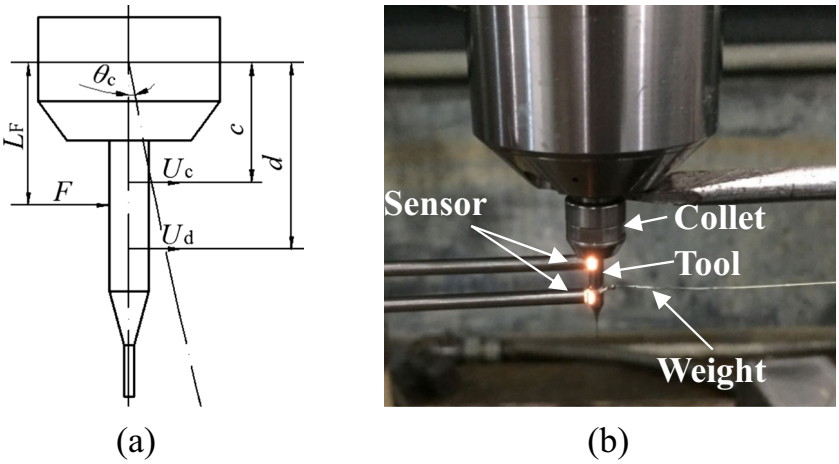

Fig. 6 Measurement diagram (**a**) and photograph (**b**) for angular stiffness of collet

where the torque M_c was obtained by the applied force F at distance L_F and the angle θ_c was obtained by the measured displacements u_c at distance c and u_d and distance d. The related measured data was summarized in Table 2.The experimental angular stiffness of the collet was 195.0 N·m/rad. To obtain the radial offset of tool tip, the angular stiffness was transformed into equivalent radial stiffness. Given that the distance from the tool tip to the center of collet L_t was 25 mm in experiment, the equivalent radial stiffness $k_{c\theta}$ was given by Eq. (6). Accordingly, the equivalent radial stiffness in this study is 312.0 mN/μm, which is far smaller than the radial stiffness.

$$k_{C\theta} = \frac{k_\theta}{{L_t}^2} \tag{6}$$

2.1.3 Stiffness of micro-spindle

The spindle rotor of micro-spindle is supported by angular contact ball bearings. Due to the integrality of the micro-spindle, there is no need to differentiate the stiffness of the rotor from that of the bearings. Their integral stiffness (i.e., stiffness of the micro-spindle) was measured by applying a load on the spindle rotor. A maximum displacement of 0.37 μm was obtained at a load of 2 N. The stiffness of the micro-spindle is 5480.0 mN/μm. It should be noted that the micro-spindle was mounted onto the conventional jig grinding machine. The measured stiffness can be approximated to the stiffness of micro-spindle due to the large size and high stiffness level of the machine tool.

Table 2 Parameters for calculation of angular stiffness of collet

Measurement parameters (mm)	Load F (N)	Displacement u_c (μm)	Displacement u_d (μm)
$c = 7.5$	2.0	0.15	0.30
$L_f = 14$	2.5	0.20	0.40
$b = 16$	3.0	0.25	0.50
	3.5	0.35	0.70
	4.0	0.45	0.90

2.2 Thermally induced error

The micro-spindle is driven by an air turbine, which generates extremely low amount of heat. However, the friction of ball bearings generates more heat. Although the ball bearing can be cooled by airflow, thermal growth may occur, which results in the axial and radial error of spindle rotor and attached micro-tool. The axial error caused by spindle thermal growth was studied by Kim [19] and Creighton [15] et al., and the corresponding spindle growth models were given. However, there have been few studies reporting on the radial error of micro-spindle system. In this study, the thermal growths at front bearing which is close to the collet and rear bearing were

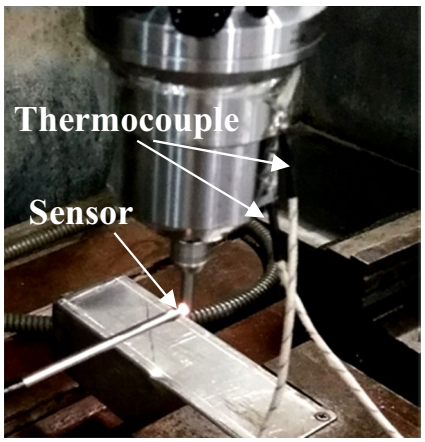

Fig. 7 Measurement of thermally induced radial error

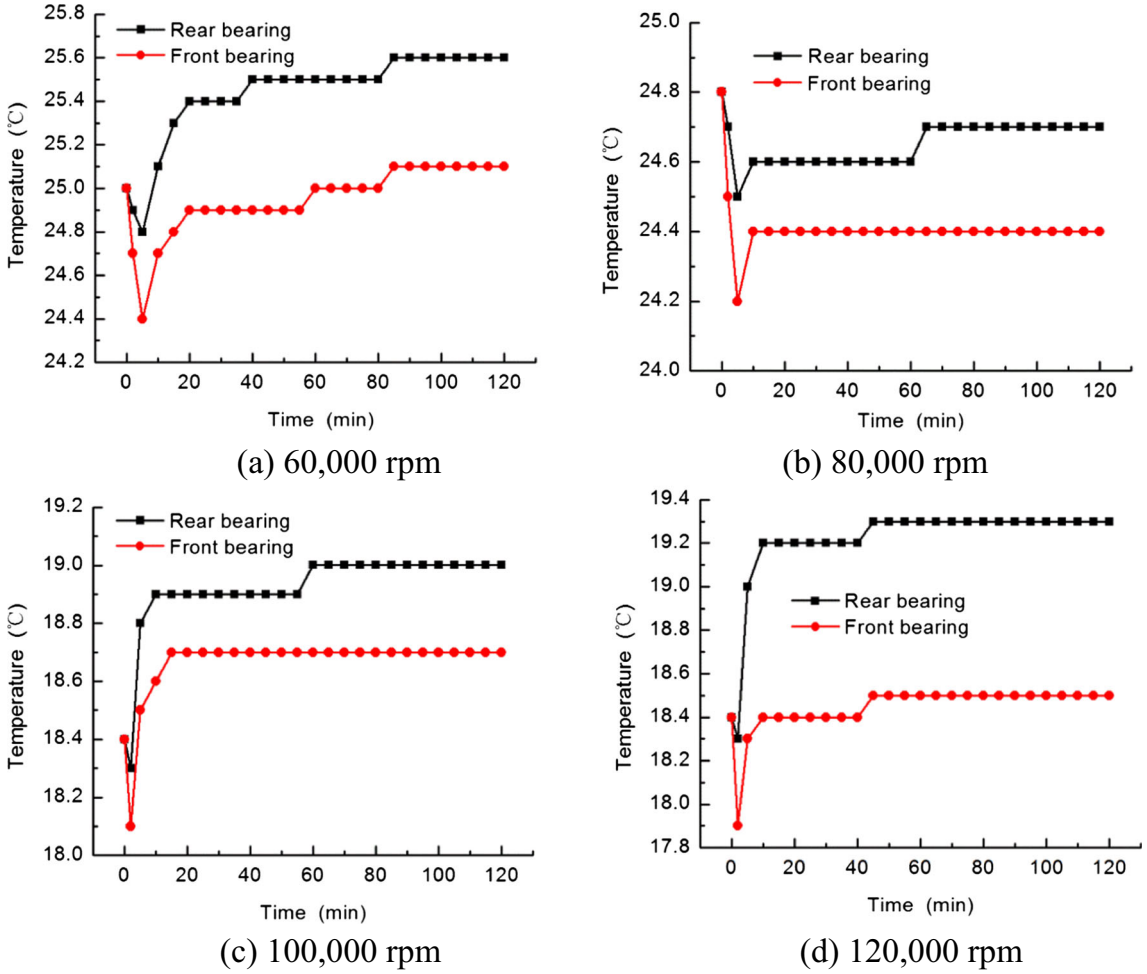

Fig. 8 **a**–**d** Temperatures of front and rear bearings at different rotational speeds

measured by thermocouples, as shown in Fig. 7. The measured temperatures are not the actual temperatures of the front and rear bearings. However, they can reflect the thermal growths of two bearings to some extent and thus qualitatively explain the thermally induced error of micro-spindle. It is worth noting that the low rotation speeds of air turbine micro-spindle are seldom used due to large speed loss at low air pressure. In addition, the ultra-high rotational speeds such as 140,000–150,000 rpm are difficult to achieve due to the cutting load and performance degradation after long-term use. Therefore, the thermally induced error at rotational speeds of 60,000–120,000 rpm (corresponding to air pressures of 0.2–0.5 MPa) was analyzed.

Figure 8 shows the temperatures at different rotational speeds. The temperatures of the front bearing and the rear bearing both went down to a minimum within the first 5 min and then rose up, which is attributed to the airflow cooling. The airflow goes past the flow channel and cools the bearings nearby. At the beginning, the heat generation from the bearings is very small and the airflow can effectively lower the temperature. With the running of the spindle, the heat amount gradually increases, and the temperature consequently begins to rise and finally remains to be stable. Unlike ball-bearing electric micro-spindles [16], this micro-spindle's temperature does not increase with the rotational speed. The stable temperature of front bearing decreased with the increasing

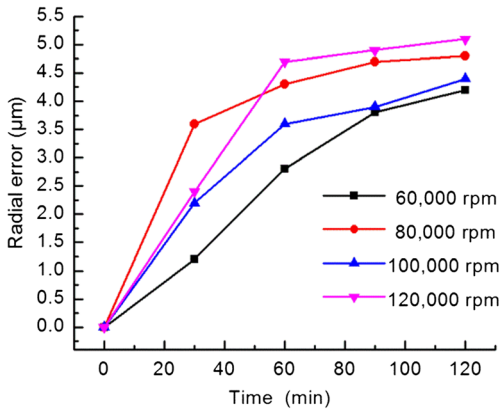

Fig. 9 Thermally induced radial errors of micro-tool tip at various rotational speeds

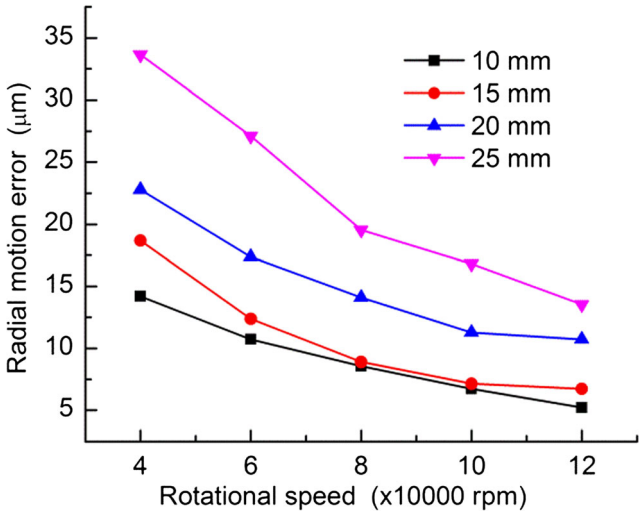

Fig. 10 Radial motion errors of micro-tool tip

rotational speed. However, the stable temperature of rear bearing did not follow such change law because of the influence of airflow change. With the increasing rotational speed, more heat is generated from the bearing, and the air pressure and airflow are also increased. Therefore, its cooling action intensifies and the temperature does not progressively increase. In addition, the temperature of the front bearing was lower than that of the rear bearing, which is due to airflow cooling efficiency. All the airflow outlets of the micro-spindle are located in the free conical end and near the front bearing, which makes the front bearing receive more thermal loss.

The thermal growth discrepancy between the front and rear bearings may result in the radial errors of the spindle rotor and attached micro-tool. To validate this inference, the radial error of micro-tool tip was measured by MTI-2100 fotonic sensor, as shown in Fig. 7. The micro-tool was replaced by a cylindrical artifact, and the same point of artifact tip was measured to obtain accurate radial error of micro-tool tip. To exclude the radial motion error of the micro-spindle, the radial error was measured after the micro-spindle stopped, and each measurement was completed as quickly as possible to minimize the effect of thermal dissipation. Thereby, the measured radial error can be regarded as thermally induced radial error of the micro-tool tip. Figure 9 shows the measured thermally induced radial error of the micro-tool tip at different rotational speeds. It is obvious that the radial error increases rapidly with running time within the first hour. Subsequently, the increasing rate is gradually lowered and finally enters into a stable state. The maximum radial errors for 60,000, 80,000, 100,000, and 120,000 rpm are 4.2, 4.8, 4.4, and 5.1 μm, respectively. Moreover, there is no positive or negative relation between the thermally induced radial error and rotational speed, which is different from the ball-bearing electric micro-spindle. The temperature change is caused by the interaction between airflow cooling and bearing frictional heating. The effect of airflow cooling on the front bearing is different from that on the rear bearing. As a result, the temperature difference between front bearing and rear bearing does not increase or decrease with the rotational speed, as shown in Fig. 8. Accordingly, a positive or negative relation between the radial error and rotational speed does not appear.

2.3 Radial motion error of micro-tool tip

The motion error of the micro-spindle is another important element that affects the machining accuracy and surface roughness. Although the spindle runout is within 1 μm, the radial motion error of the micro-tool tip may be larger due to the misalignment between micro-tool and collet chuck as well as the performance degradation after long-term use. Moreover, radial motion error may be aggravated by the over-hang length and the imbalance of micro-tool and collet. The micro-tool is 35 mm in overall length and 25 mm in tool body length, as shown in Fig. 2. Given that the minimum

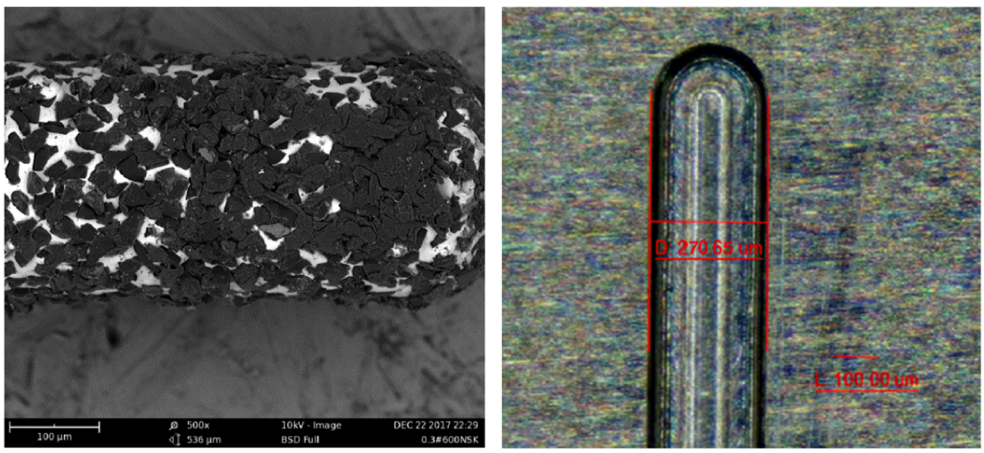

Fig. 11 Micro-grinding tool (**a**) and machined micro-slot (**b**)

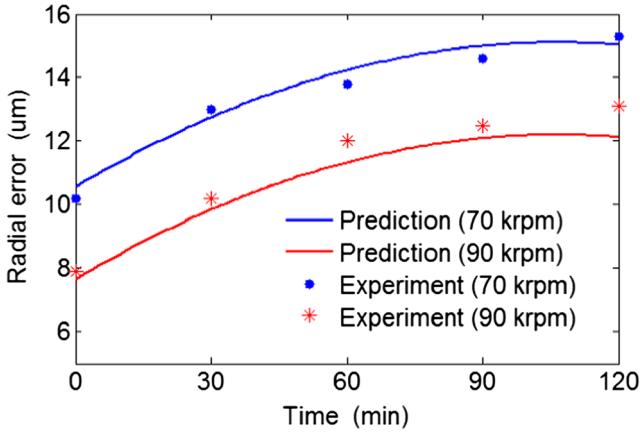

Fig. 12 Comparison of experimental and predicted radial errors

clamping length is 10 mm, the over-hang length of the micro-tool ranges from 10 to 25 mm. Therefore, experiments on the radial motion error of the micro-tool tip with over-hang lengths of 10, 15, 20, and 25 mm were performed at rotational speeds ranging from 40,000 to 120,000 rpm. In the experiments, the measurements were completed as quickly as possible to exclude the influence of thermally induced error.

Figure 10 shows the radial motion errors of the micro-tool tip measured by MTI-2100 fotonic sensor. The radial motion error of the tool tip decreases with the rotational speed. For an over-hang length of 15 mm, the radial motion error was about 18.7 μm at a rotational speed of 40,000 rpm. As the rotational speed increased to 60,000, 80,000, 100,000, and 120,000 rpm, the radial motion error decreased to 12.4, 8.9, 7.2, and 6.7 μm, respectively. The radial motion error of the tool tip increased with over-hang length of micro-tool. At a rotational speed of 80,000 rpm, the radial motion errors were 8.6, 8.9, 14.1, and 19.5 μm for the over-hang lengths of 10, 15, 20, and 25 mm, respectively. Accordingly, to decrease the radial motion error of the micro-tool tip, the over-hang length should be short as possible. On the other hand, the micro-tool needs to have certain over-hang length in order to machine miniature workpiece with deep micro-feature, such as micro-wall and micro-cylinder. As shown in Fig. 10, the decreasing range of radial motion error gradually became small with the decreasing over-hang length. For instance, the radial motion error of micro-tool with over-hang length of 15 mm was not much bigger than that with over-hang length of 10 mm, especially within rotational speed from 60,000 to 120,000 rpm. Therefore, considering the radial motion error and requirement of machining range, the over-hang length of 15 mm was adopted in the micro-grinding experiments below.

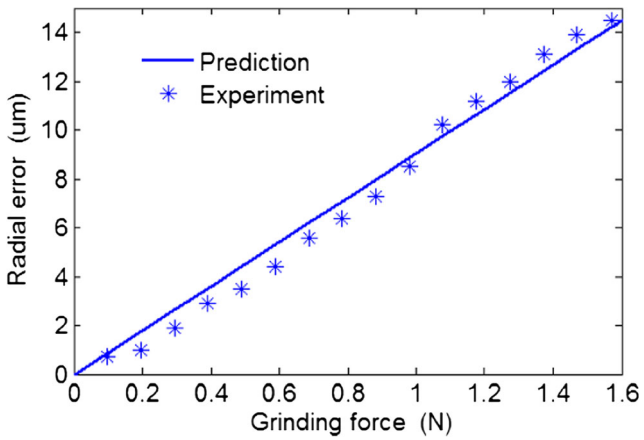

Fig. 13 Comparison between experimental and predicted radial offsets caused by grinding force

3 Error compensation strategy

According to above analysis, the radial error of the micro-tool tip ΔU is a comprehensive embodiment of mechanical offset ΔU_s, thermally induced error ΔU_t, and radial motion error ΔU_m. The mechanical offset ΔU_s can be calculated by

$$\Delta U_s = \frac{F_r}{K_g} = F_r\left(\frac{1}{k_{sp}} + \frac{1}{k_c} + \frac{1}{k_t}\right) \tag{7}$$

The predictive model of thermally induced error can be obtained by fitting measured radial errors, as shown in Fig. 9. It can be seen that the radial error has a quadratic function relationship with the time. With the increase of rotation speed, the thermally induced error shows a changing tendency of increasing first, and then falling, increasing again, and then falling again; therefore, the sine function was used to simulate their relationship. The mean values of radial errors were regarded as target values, and the relationship between thermally induced error and time was fitted using the least square method with the software Matlab. Since the spindle thermal growth is exponential in nature [15, 19], this law also accounts for the thermally induced radial error. Accordingly, the predictive model of thermally induced error ΔU_t is expressed as

$$\Delta U_t = -4*10^{-4}t^2 + 853*10^{-4}t + 143*10^{-4} + 1.5\sin(1.001-e^{-t})*\sin\left(-0.5*10^{-4}\pi n + 4.5\pi\right) \tag{8}$$

where t is time (min) and n is rotational speed (rpm).

The calculation results obtained according to Eq. (8) have a large fitting error near 30 min. Nevertheless, the coefficient of determination R^2 is 0.96, which indicates a good fitting of the thermally induced error with the time and rotational speed.

The radial motion error of micro-tool tip with an over-hang length of 15 mm is showed in Fig. 10. The fitting between the radial motion and rotational speed was conducted according to least square method with the software Matlab. The predictive

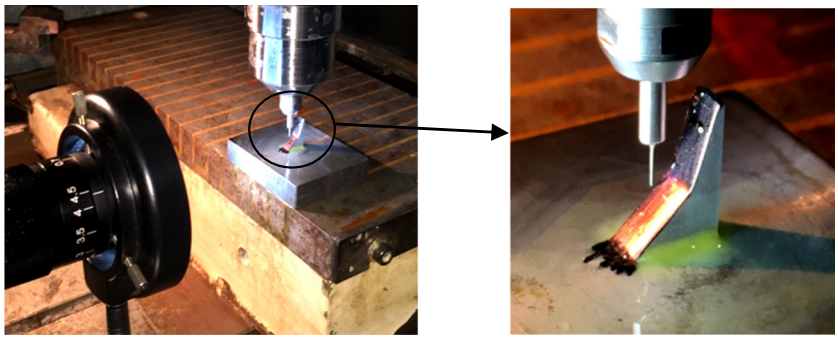

Fig. 14 Micro-grinding of duralumin 6061

model is given by Eq. (9). The coefficient of determination R^2 is 0.99, which indicates a good fitting between the radial motion error and rotational speed.

$$\Delta U_{\mathrm{m}} = 24.02{*}10^{-10}{*}n^2 - 52.96{*}10^{-5}{*}n + 35.84 \quad (9)$$

It was worth noting that the motion error in actual machining may be smaller than that at idling running, which was verified by micro-grinding of micro-slot, as shown in Fig. 11. The tip diameter of the micro-grinding tool was 261.7 μm, whereas the width of the machined micro-slot at a rotational speed of 60,000 rpm was 270.7 μm. This meant that the width difference of 9.0 μm was resulted from the radial motion error of the micro-grinding tool tip. However, according to Fig. 10, the radial motional error of the tool tip was 12.4 μm, which was larger than that of actual micro-machining. The micro-grinding process, which is usually applied to single-side grinding, has small effect on radial motion error compared with micro grinding of micro-slot. Therefore, the proposed predictive model (Eq. 9) can be used for the prediction of radial motion error of micro-tool tip.

4 Experiments and verifications

The radial errors of the micro-grinding tool tip were measured and compared with results predicted by the model, as shown in Fig. 12. The micro-spindle was at idling running state, so the mechanical offset was not included. It can be seen that the experimental maximum radial error exceeded 10 μm, which verifies the necessity of error compensation of ultra-high micro-spindle system in mechanical micro-machining. The predicted radial error had a maximum deviation of approximately 1 μm, which agreed well with the experimental data.

Figure 13 depicts the experimental and predicted radial offsets of the micro-grinding tool tip caused by grinding forces. The predicted values agreed well with the experimental results.

The error compensation was used in micro-grinding of duralumin 6061, as shown in Fig. 14. The error compensation was fulfilled by real timely moving the worktable in this study. The machined workpiece has two planes inclined at 75° and 45°, respectively. To achieve exact tool adjustment, the micro-grinding tool firstly approached as close as possible to the workpiece and then slid along the workpiece, and the whole process was monitored by the industrial microscope JT-1400B. The tool adjustment was not completed until some bright traces were found in the workpiece. Subsequently, the side micro-grinding was carried out at a rotational speed of 60,000 rpm, and the actual grinding depth was measured as shown in Fig. 15. Due to the radial motion error of the micro-grinding tool, one surface was machined at 45°-inclined plane, with actual grinding thickness reaching 5.6 μm. Then, under the grinding thickness of 30.0 μm, two surfaces were machined at 45°-inclined and 75°-inclined planes, respectively. The actual grinding thickness at 45°-inclined plane was 33.2 μm, which was larger than that at 75°-inclined plane by around 1.1 μm. Through experiment,

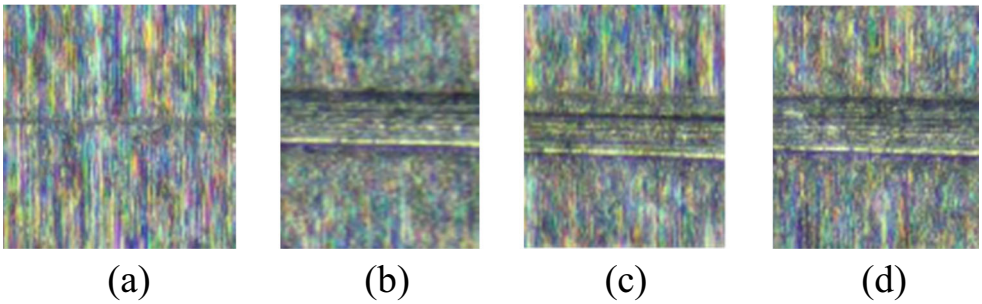

Fig. 15 Machined micro-faces. **a** No grinding thickness at 45°-inclined plane, **b** 30-μm grinding thickness at 45°-inclined plane, **c** 30-μm grinding thickness at 75°-inclined plane, and **d** error compensation at 45°-inclined plane

the tool radial offset caused by grinding force has been verified to have an important effect on the mechanical micro-machining. The predicted tool offset at a grinding force of 0.3 N was 2.7 μm whereas the predicted radial error was 5.7 μm. It should be noted that the radial offset of micro-grinding tool tip reduces the machining amount, whereas thermally induced error and motion error enlarge the machining amount. Thereby, the grinding thickness should be reduced by 3.0 μm. With this error compensation, a side surface was machined at 45°-inclined plane, with actual grinding thickness of about 30.7 μm, which shows the machining error was reduced to 0.7 μm.

5 Conclusions

The radial error of a high-speed precision micro-spindle system equipped with micro-tool was deeply analyzed in this study, and the following conclusions were drawn:

1. The radial error of micro-tool tip is a comprehensive embodiment of mechanical offset, thermally induced error, and motion error. In side micro-machining, the mechanical offset reduces the actual thickness whereas the thermally induced error and motion error enlarge the actual thickness.
2. The micro-tool tip, having the smallest stiffness, is the major error source of radial mechanical offset. The angular stiffness of collet should be also concerned. Its equivalent radial stiffness is 312.0 mN/μm, which is larger than that of micro-tool tip by 117 mN/μm. The radial stiffnesses of micro-tool body, collet, and micro-spindle are far larger than the radial stiffness of micro-tool tip and equivalent radial stiffness of collet.
3. The temperatures of two bearings went down to a minimum within the first 5 min due to air cooling and then gradually rose up. Since higher rotational speed demands higher air pressure and thus brings better cooling effect, this air-turbine micro-spindle's temperature does not increase with the rotational speed, which is different from the ball-bearing electric micro-spindle. The front bearing receives more thermal loss and thus had lower temperature than the rear bearing at nearly all rotational speeds.
4. The different thermal growths between two ball bearings of the micro-spindle result in the thermally induced error. The thermally induced error increased rapidly with running time within the first hour and then entered into a relative stable state. In addition, there is no positive or negative relationship between thermally induced error and rotational speed due to different airflow cooling effects on the front and rear bearings.
5. The radial motion error increased with the over-hang length of micro-tool, but decreased with the rotational speed. To reach a balance between the machining range and accuracy, an over-hang length of 15 mm was adopted and its maximum radial motion error was 12.3 μm at a rotational speed of 60,000 rpm. As subjected to machining load, the radial motion error of micro-tool tip in actual micro-machining is normally smaller than that at idling running state.
6. The radial mechanical offset, thermally induced error, and motion error of micro-tool tip predicted by the proposed error models were in good consistent with the measured values, which showed good reliability of the proposed models. The micro-grinding tests also verified the rationality of the proposed models. With the error compensation, the experimental micro-grinding thickness was close to the required value. This indicated the error compensation scheme improved micro-machining accuracy greatly.

Funding information The presented work is funded by the National Science Foundation of China (51505140, 51675170), China Postdoctoral Science Foundation (2016T90749, 2015M570676), and Natural Science Foundation of Hunan Province, China (2016JJ3037).

References

1. Uhlmann E, Mullany B, Biermann D, Rajurkar KP, Hausotte T, Brinksmeier E (2016) Process chains for high-precision components with micro-scale features. CIRP Ann Manuf Technol 65: 549–572. https://doi.org/10.1016/j.cirp.2016.05.001
2. Pratap A, Patra K, Dyakonov AA (2016) Manufacturing miniature products by micro-grinding: a review. Procedia Eng 150:969–974. https://doi.org/10.1016/j.proeng.2016.07.072
3. Dornfeld D, Min S, Takeuchi Y (2016) Recent advances in mechanical micromachining. CIRP Ann Manuf Technol 55:745–768. https://doi.org/10.1016/j.cirp.2006.10.006
4. Huo DH, Cheng K (2013) Overview of micro cutting. In: Micro-cutting: fundamentals and applications. Wiley, Chichester, pp 1–17. https://doi.org/10.1002/9781118536605.ch1
5. Ehmann KF, DeVor RE, Kapoor SG, Cao J (2008) Design and analysis of micro/meso-scale machine tools. In: Smart Devices Mach Adv Manuf. Springer, London, pp 283–318. https://doi.org/10.1007/978-1-84800-147-3_12
6. Müller C, Kirsch B, Aurich JC (2017) Compact air bearing spindles for desktop sized machine tools. In: Small machine tools for small workpieces. Springer, Cham, pp 21–34. https://doi.org/10.1007/978-3-319-49269-8_2
7. Jahanmir S, Ren Z, Heshmat H, Tomaszewski M (2010) Design and evaluation of an ultrahigh speed micro-machining spindle. Mach Sci Technol 14:224–243. https://doi.org/10.1080/10910344.2010.489406
8. Li W, Zhou ZX, Xiao H, Zhang B (2015) Design and evaluation of a high-speed and precision microspindle. Int J Adv Manuf Technol 78:997–1004. https://doi.org/10.1007/s00170-014-6690-x
9. Li W, Zhou Z, Zhang B, Xiao YY (2016) A micro-coupling for micro mechanical systems. Chin J Mech Eng 29:571–578. https://doi.org/10.3901/CJME.2016.0115.009
10. Ashok SD, Samuel GL (2012) Modeling, measurement, and evaluation of spindle radial errors in a miniaturized machine tool. Int J

Adv Manuf Technol 59:445–461. https://doi.org/10.1007/s00170-011-3519-8

11. Murakami H, Kawagoishi N, Kondo E, Kodama A (2010) Optical technique to measure five-degree-of-freedom error motions for a high-speed microspindle. Int J Precis Eng Manuf 11:845–850. https://doi.org/10.1007/s12541-010-0102-4
12. Anandan KP, Ozdoganlar OB (2013) An LDV-based methodology for measuring axial and radial error motions when using miniature ultra-high-speed (UHS) micromachining spindles. Precis Eng 37:172–186. https://doi.org/10.1016/j.precisioneng.2012.08.001
13. Bediz B, Gozen BA, Korkmaz E, Ozdoganlar OB (2014) Dynamics of ultra-high-speed (UHS) spindles used for micromachining. Int J Mach Tool Manu 87:27–38. https://doi.org/10.1016/j.ijmachtools.2013.02.005
14. Bediz B (2014) Three dimensional dynamics of micro tools and miniature ultra-high-speed spindles. Dissertation, Carnegie Mellon University
15. Creighton E, Honegger A, Tulsian A, Mukhopadhyay D (2010) Analysis of thermal errors in a high-speed micro-milling spindle. Int J Mach Tool Manu 50:386–393. https://doi.org/10.1016/j.ijmachtools.2009.11.002
16. Anandan KP, Ozdoganlar OB (2013) Analysis of error motions of ultra-high-speed (UHS) micromachining spindles. Int J Mach Tool Manu 70:1–14. https://doi.org/10.1016/j.ijmachtools.2013.02.005
17. Uriarte L, Herrero A, Zatarain M, Santiso G, Lacalle LNLD (2007) Error budget and stiffness chain assessment in a micromilling machine equipped with tools less than 0.3 mm in diameter. Precis Eng 31:1–12. https://doi.org/10.1016/j.precisioneng.2005.11.010
18. Salgado MA, Lacalle LNLD, Lamikiz A, Muñoa J, Sánchez JA (2005) Evaluation of the stiffness chain on the deflection of end-mills under cutting forces. Int J Mach Tool Manu 45:727–739. https://doi.org/10.1016/j.ijmachtools.2004.08.023
19. Kim KD, Kim MS, Chung SC (2004) Real-time compensatory control of thermal errors for high-speed machine tools. P I Mech Eng B-J Eng 218:913–924. https://doi.org/10.1243/0954405041486163